Turkish Journal of Zoology

Volume 47 | Number 1 Article 1

1-1-2023

Skeletochronology in long tubular bones of the Javan water monitor lizard, Varanus salvator bivittatus in the juvenile stage (Lacertilia: Varanidae)

HELLEN KURNIATI

NI LUH PUTU RISCHA PHADMACANTY

GONO SEMIADI

Turkish Journal of Zoology
http://journals.tubitak.gov.tr/zoology/
Research Article
Turk J Zool
(2023) 47: 1-9
© TÜBİTAK
doi:10.55730/1300-0179.3107

Skeletochronology in long tubular bones of the Javan water monitor lizard, *Varanus salvator bivittatus* in the juvenile stage (Lacertilia: Varanidae)

Hellen KURNIATI[1,*], **Ni Luh Putu Rischa PHADMACANTY**[2], **Gono SEMIADI**[1]
[1]Research Center for Ecology and Ethnobiology, National Research and Innovation Agency (BRIN), Jalan Raya Jakarta-Bogor, Cibinong Indonesia
[2]Research Center for Applied Zoology, National Research and Innovation Agency (BRIN), Jalan Raya Jakarta-Bogor, Cibinong Indonesia

Received: 02.06.2022 • **Accepted/Published Online:** 21.12.2022 • **Final Version:** 11.01.2023

Abstract: Age estimation of the juvenile stage of *Varanus salvator bivittatus* using limb bones, namely the big long tubular bones (femur, tibia, humerus) and the small long tubular bones (fibula, radius, ulna, phalanx), was performed using the skeletochronological method. Samples were from Java Island, Indonesia and provided by the pet exporters. Lines of arrested growth (LAG) were present and the first growth mark was visible on a female with a snout-vent length (SVL) of 18.8 cm, and a male with SVL of 19.3 cm. The process of resorption begins in the juvenile stage, and resorption occurs in all long tubular bones. Inside the big long tubular bones, resorption begins earlier and is more extensive than in the small long tubular bones, and in one individual with SVL 25.0 cm, the endosteal bone had completely eroded in all big tubular bones. Resorption also occurred in the small long tubular bones; however, on one individual with an SVL of 25.0 cm, the remaining endosteal bone was still visible only in fibula bone. Linear regression analysis resulted in a weak correlation, statistically insignificant between the SVL and the diameter of the marrow cavity (d) in the fibula bone, while in other bones the correlations were strong and statistically significant ($p < 0.005$). Among seven tubular bones, the resorption rate in the fibula bone was the lowest but very high in the phalanx bone. Radial osteon formation has occurred in the smallest individual with SVL 14.4 cm to the biggest one with SVL 25.0 cm, and radial osteon density increases with increased SVL. There was no radial osteon in fibula and phalanx bones in any sampled specimen. In general, there were no significant differences in bone diameter (D), marrow cavity diameter (d) and bone thickness (MP) in all long tubular bones in both male and female individuals, and the density of radial osteon on some tubular bones was influenced by body length, but not by sex.

Key words: Common water monitor, *Varanus salvator bivittatus*, histology, Indonesia, Java Island, limb bones

1. Introduction

The common water monitor lizard (*Varanus salvator)* has a wide distribution throughout southern Asia and southeast Asia (Bennett, 1998; Quah et al., 2021). In Indonesia, it is known from Sumatra, Java, Kalimantan, Sulawesi and their nearby islands, the Lesser Sunda Islands, and on several islands in the Moluccas (Quah et al., 2021). According to Koch et al. (2010), there are three subspecies of *V. salvator* in Indonesia, i.e. *V.s. macromaculatus* in Sumatra and Kalimantan, *V.s. bivittatus* in Java and adjacent islands, and *V. s. ziegleri* in Sulawesi. These subspecies of *V. salvator* are not among the species of protected wildlife in Indonesia. At present, the common water monitor is included in the IUCN 'Least Concern' (LC) category (Quah et al., 2021).

The common water monitor is a highly exploited lizard in Indonesia (Shine et al., 1996; 1998), where the lizard is utilized for its skin, meat, fat, and as live individuals for the pet trade. Utilization of common water monitors for pets in Indonesia is mostly (about 95%) in the juvenile stage. There is rarely a demand for the international buyers of older and larger individuals (Andre van Meer, personal communication). Harvesting from the wild for international trade is regulated through an annual quota mechanism, based on the recommendations of the Indonesian Scientific Authority c/q National Research and Innovation Agency (BRIN). Despite the prevalence of the common water monitor in Indonesia, aspects of *V.s. bivitattus* biology (e.g., bone growth) are not well understood.

Long tubular bone growth is a dynamic process in which bone deposition and bone resorption occur simultaneously. Bone resorption generally occurs along the marrow cavity. After resorption, endosteal bone is deposited and separated from primary bone by a resorption line (RL; Kurita and Toda, 2013; Kumas and Ayaz, 2014; Bulbul et al., 2016; Uzum et al., 2014, 2015,

* Correspondence: hellenkurniati@gmail.com

2018). On the other hand, bone deposition typically occurs on the periosteal surface and pauses in bone growth result in growth mark formation. For example, lines of arrested growth (LAG) form due to annual pauses in bone growth and can be used in aging individuals (i.e. skeletochronology), and additional resting lines (AdL) can form due to brief nonannual pauses in growth.

The skeletochronological method is commonly used to estimate the age of amphibians and reptiles by observing the presence of annually formed LAG (Francillon-Vieillot et al., 1990) in bone cross section. Counting annual growth marks is very effective and applicable in estimating the age of various reptilian species (e.g., Castanet, 1994; Kurita and Toda, 2013), though additional nonannual growth marks or AdL can also occur (e.g., Smirina and Ananjeva, 2017; Kurniati and Phadmacanty, 2022). Age estimation of varanid lizards using the skeletochronology method has been carried out on *Varanus griseus*, which is found in temperate regions (Smirina and Tsellarius, 1996; 1998), and *V. niloticus*, a varanid species that lives in tropical Africa (De Buffrinil and Castanet, 2000). However, age estimations of *V. salvator* in the Asian region have not been carried out yet. Before this skeletochronology study proceeds to a group of adult individuals, the skeletochronology of juvenile *V.s. bivittatus* was examined. This study aims to assess the long tubular bone condition, evaluate the extent of bone resorption in the long tubular bones, and investigate growth marks (both annual and nonannual) in the bone cross-sections of juvenile V.s. *bivittatus*.

2. Materials and methods

2.1. Ethics statement

All of bone samples were collected from juvenile stage individuals that were already dead in the PT. Mega Citrindo reptile farm in Jakarta, Indonesia. No individual of *V.s. bivittatus* were intentionally killed for this study.

2.2. Specimens

Long tubular bones of forelimb and hindlimb (phalanx, tibia, fibula, femur, humerus, radius and ulna) were selected from dead specimens of juvenile *V.s. bivittatus* in the PT. Mega Citrindo reptile farm in Jakarta, Indonesia. The specimens were all wild caught and originated from Central Java Province, Indonesia. Before the lizards were dissected for sexing, snout-vent length (SVL) was measured. After that, the femur, tibia, fibula, humerus, radius, ulna, and second phalanx from the longest finger (digit II) in right forelimb and hindlimb were taken. A total of 21 individuals (10 males, 11 females) were used in this skeletochronology study.

2.3. Skeletochronology

All long tubular bones of forelimb and hindlimb were used for the skeletochronology study, and the steps of bone processing followed Sinsch (2015). The bones were decalcified by using 10% formic acid for 2–15-h, depending on the size of the bones. All bones were stained with Erlich's hematoxylin for 90 min. Following Comas et al. (2016), 20 µm of transverse sections were prepared using a freezing microtome (Yamato RV - 240, Japan). For each tubular bone, at least three good cross sections were selected at the middiaphyseal part with the smallest marrow cavity. For the histological processes, all cross sections were mounted by entellan and analyzed by a compound microscope (Nikon Optiphot 2, Japan) and attached to a computer for photographic analysis. LAGs were identified as growth marks of annual cyclicity of the shaft bone (Woodward et al., 2013), whereas nonannual resting lines were identified as AdLs. The thickest width of bone from the edge of the marrow cavity to the periosteal outer margin (MP), the longest distance of diameter (D), and the greatest diameter of the marrow cavity (d) were measured by using ImageJ version 1.53 (Schneider et.al., 2012) (Figure 1).

2.4. Data analyses

To evaluate the extent of resorption in each bone, the PAST software (Hammer et al., 2001) was used to analyze data from measured parameters (MP, D, d, SVL) within each sex; however, all the measurement parameters were analyzed across the entire sample regardless of specimen age. All measurement data were transformed to logarithmic values for linear regression analysis. Statistical correlation was used to identify the correlation between SVL with D, MP, and d, respectively. The extent of resorption was calculated by dividing D and "d" in all bones. The ANOVA Kruskal–Wallis test was used to test whether the measured parameters (D, d, MP and SVL) were significantly different between males and females at level $p < 0.05$.

3. Results

The seven long tubular bones of the forelimb and hind limb that were used in this study can be divided into two groups, based on the size of the bone diameter, namely the big long tubular bones, consisting of the femur, tibia, and humerus; and the small long tubular bones, which consisted of the fibula, radius, ulna, and phalanx. Generally, the shape of the long tubular bones in cross section is circular, except the ulna, which is oval, and phalanx, which has a horseshoe shape. The first LAG in males appeared in an individual with SVL of 19.3 cm and in females with SVL of 18.8 cm. A second LAG appeared in all bone cross section of a single female specimen with SVL of 25.0 cm (Table 1); however, the second LAG is still in question due to the short distance between the two LAGs.

The microanatomy of the cross sections of the femur, tibia, fibula, humerus, radius, ulna, and phalanx of *V.s. bivittatus* consisted of radial osteons within woven fibered

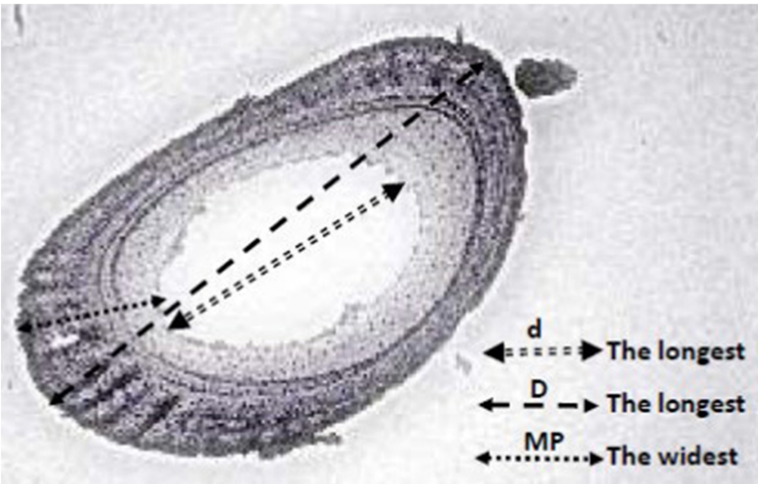

Figure 1. Measurement of bone cross section. d: the longest part of the marrow cavity; D: the longest part of the bone diameter; MP: the widest point of bone thickness.

Table 1. Density of radial osteon in each tubular bone on 10 individual males and 11 individual females of juvenile *V.s. bivittatus*. low density (+), intermediate density (++), high density (+++), very high density (++++), none (-).

Sex	SVL (cm)	Number of LAG	Femur	Tibia	Humerus	Fibula	Radius	Ulna	Phalanx
Male 1	14.4	0	+	+	+	-	-	-	-
Male 2	15.4	0	++	+	++	-	-	-	-
Male 3	16.1	0	++	+	++	-	-	-	-
Male 4	17.8	0	+++	++	+++	-	-	+	-
Male 5	17.9	0	++	-	++	-	-	+	-
Male 6	18.5	0	+++	++	+++	-	-	+	-
Male 7	18.9	0	+++	++	++	-	+	+	-
Male 8	19.3	1	++++	+++	++++	-	+	+	-
Male 9	20.0	0	++++	+++	++++	-	+	+	-
Male 10	22.2	1	++++	+++	++++	-	+	+	-
Female 1	15.1	0	++	+	++	-	-	-	-
Female 2	15.4	0	++	+	++	-	-	-	-
Female 3	15.5	0	+	+	+	-	-	-	-
Female 4	15.8	0	+++	+	+	-	-	-	-
Female 5	16.8	0	++	++	++	-	-	+	-
Female 6	17.1	0	++	++	++	-	+	+	-
Female 7	17.2	0	+++	++	++	-	+	+	-
Female 8	17.5	0	+++	++	++	-	+	+	-
Female 9	18.8	1	++++	++	++++	-	+	+	-
Female 10	22.2	1	+++	++	++++	-	+	+	-
Female 11	25.0	2 (?)	++++	++	++++	-	+	+	-

cortical tissue and an innermost layer of endosteal bone, consistent with Buffrenil and Castanet (2000). Radial osteon density is variable across the sampled bones and between individuals (Table 1 and Figures 2 and 3).

Radial osteon density was not quantified. Instead, bones were assessed subjectively and categorized from low density (+) (infrequent osteons) to very high density (++++) in order to compare radial osteon proliferation between bones and individuals (Table 1). For example, the radial osteons in an individual with SVL of 14.4 cm (male 1; 0 LAG) are found infrequently in the femur, tibia, and humerus (Figure 2); the radial osteon density on this individual was categorized as low density (+). As the SVL increases in individuals with SVL 22.2 cm (female 10; 1 LAG), the radial osteons multiply in the femur, tibia and humerus, and begin to appear in the radius and ulna bones (Figure 3); the radial osteon density in tibia, femur, and humerus bones were categorized as intermediate density (++), high density (+++), and very high density (++++), respectively (Table 1). The cross sections of the fibula and phalanx bones do not show radial osteon formation in any of the sampled specimens. The radial osteons have appeared in early juvenile stage individual (Figure 2), in which the long tubular bones are still predominantly of endosteal bone.

Endosteal bone appears to be eroded as the SVL length increases (Figure 3). Endosteal bone resorption occurs in all seven types of tubular bone and is defined by the decreasing of the endosteal bone (Figures 2 and 3). Endosteal bone in the big long tubular bones (femur, tibia, and humerus) has a higher extent of resorption compared to the small tubular bones (fibula, radius, and ulna); however, endosteal bone in the phalanx has the highest resorption among the small long tubular bones.

The fibula bone of a female with SVL of 25.0 cm (Figure 4) has an AdL in the endosteal bone, the AdL appearance is not found in other bones. The AdL appeared between the resorption line and the marrow cavity. However, AdLs inside the endosteal bone did not occur in other small long tubular bones (radius, ulna, and phalanx). In a female with SVL of 25.0 cm, endosteal bone was still visible, even though it had been significantly eroded. However, in the big long tubular bones, the endosteal bone had been eroded due to the resorption process.

3.1. Measurement analyses

Based on the ANOVA Welch test, there were no significant differences in the diameters of the big long tubular bones between male and female individuals (Welch F test in the case of unequal variances; $p > 0.05$), as well as the diameter of the marrow cavity (d) and the thickness of the bones (MP). The comparison of the diameters of the seven bones in all individuals is shown in Table 2.

All of the linear regression results of SVL versus D in long tubular bones resulted in a very strong correlation,

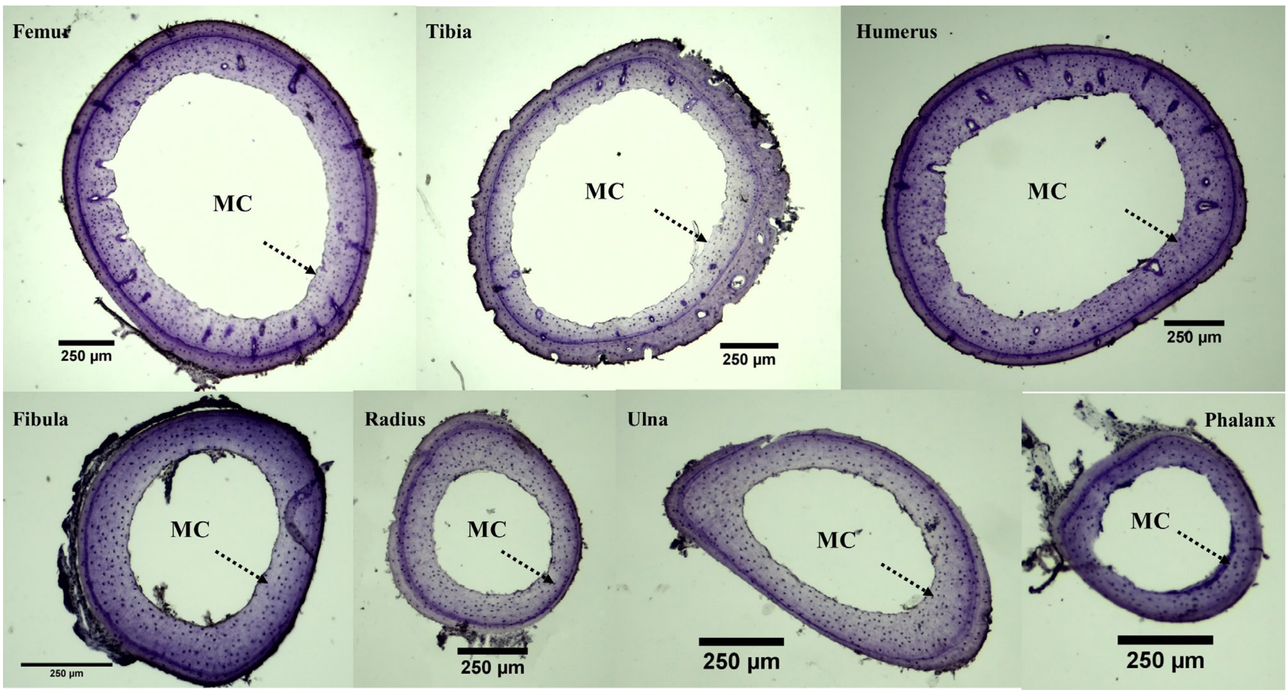

Figure 2. Cross section of the seven long tubular bones of juvenile male *Varanus salvator bivittatus* with zero LAG (SVL: 14.4 cm). MC: marrow cavity; dotted arrow: endosteal bone.

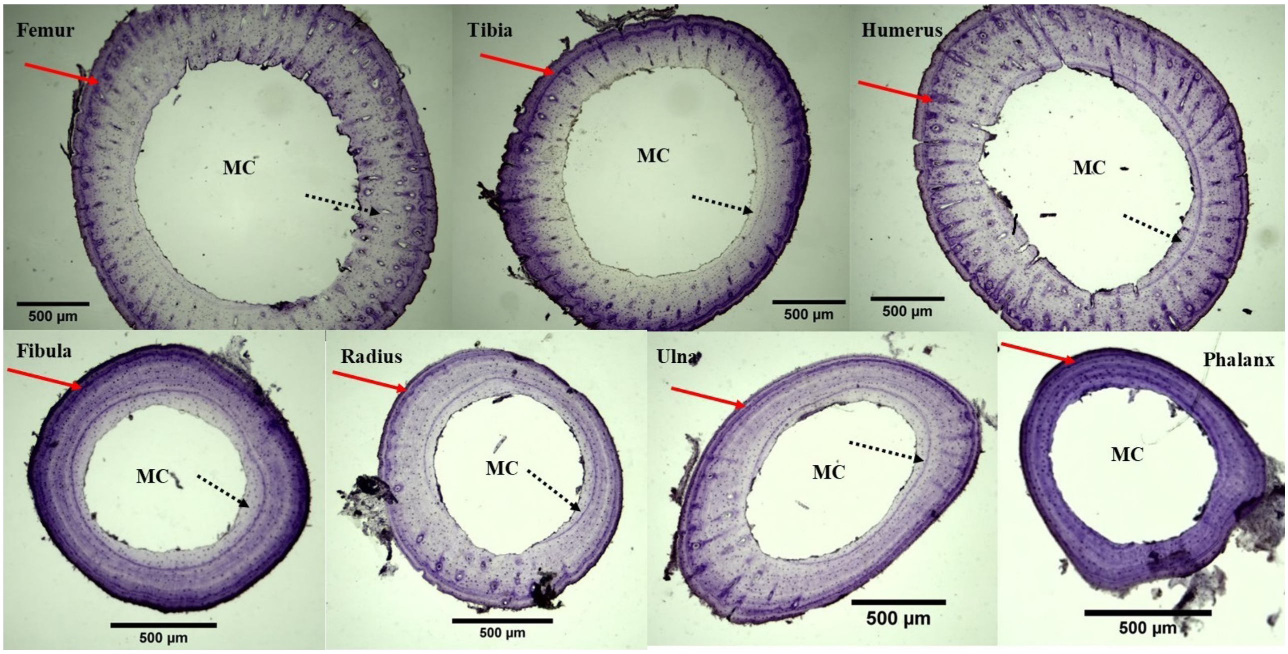

Figure 3. Cross section of the seven long tubular bones of a juvenile female *Varanus salvator bivittatus* with one LAG (SVL: 22.2 cm). MC: marrow cavity; dotted arrow: endosteal bone; red solid arrow: LAG.

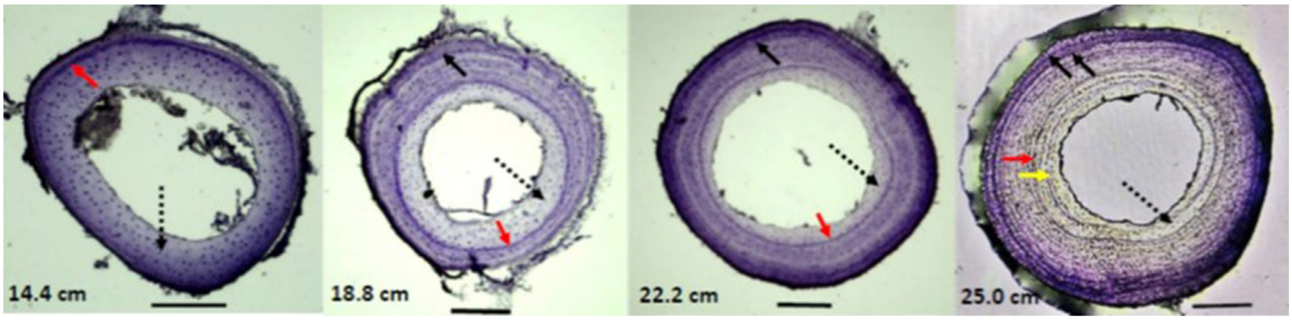

Figure 4. Cross sections of the diaphysis fibula bone in four individuals with SVLs between 14.4 cm to 25.0 cm. Dotted arrow: endosteal bone; black solid arrow: LAG; red solid arrow: resorption line (RL); yellow solid arrow: additional resting Line (AdL). The scale bar is equal to 200 m.

with $r^2 > 0.80$ ($p < 0.05$) for big long tubular bones and $r^2 \geq 0.92$ ($p = 0.0001$) for small long tubular bones (Table 3).

The average quotient between D and d showed that the resorption rates in the phalanx and tibia bones are the highest, which is equal with the lowest value among the bones; however, in the radius, ulna and fibula bones, the rate is low with a value of around 1.7 (Table 4).

4. Discussion

Osteohistological analysis, using methods by Sinsch (2015), of *V. s. bivittatus* bones revealed the existence of LAGs and RL. LAGs were clearly visible in the femur, tibia, humerus, fibula, radius, and ulna, but less clear in the phalanx (Figure 3). The first LAG appeared on female individual with SVL 18.8 cm and 22.2 cm, while on male individual with SVL 19.3 cm and 22.2 cm (Table 1). This appearance of first LAG suggests that during the juvenile stage of this varanid, sexual dimorphism has not occurred yet (Smirina and Tsellarius, 1996; De Buffrinil and Castanet, 2000; Frynta et al., 2010).

The process of resorption in endosteal bone occurred in all long tubular bones, which have different extent of resorption for each type of bone (Figures 2 and 3). This condition also occurs in the long tubular bones of the hind limb (femur, tibia, fibula, and phalanx) of *V. niloticus* (De Buffrinil and Castanet, 2000). The condition of the phalanx of the *V.s. bivittatus* was very different from the condition of the phalanx of *V. griseus* (Smirina and Tsellarius, 1996), in which the phalanx can be used for age estimation. However, in the present study, extensive resorption in *V.s.*

Table 2. Descriptive statistics on snout to vent length (SVL, cm) and measurement of long tubular bones, i.e. bone diameter (D, µm), marrow cavity diameter (d, µm), and bone thickness (MP, µm) of juvenile *V.s. bivittatus* (n = number of individuals; SD = standard deviation).

Item of measurement	Males (n = 10)	Females (n = 11)
SVL – cm		
Mean ± SD (range)	18.10 ± 2.30 (14.40–22.20)	17.85 ± 3.26 (15.10–25.00)
FEMUR		
D : Mean ± SD (range) -	2108.24 ± 382.10 (1579.39–2871.37)	1999.64 ± 458.323 (1489.32 - 2916.94)
d : Mean ± SD (range) - µm	1357.91 ± 150.38 (1118.44–1621.75)	1323.37 ± 250.85 (1097.76–1921.00)
MP : Mean ± SD (range) - µm	431.58 ± 165.5 (239.20–793.45)	386.57 ± 142.78 (192.93–589.02)
TIBIA		
D : Mean ± SD (range) -	1719.63 ± 243.39 (1413.73–2075.15)	1619.25 ± 418.00 (1221.30–2407.15)
d : Mean ± SD (range) - µm	1136.39 ± 110.57 (912.30–1260.63)	1094.92 ± 224.72 (853.10–1586.77)
MP : Mean ± SD (range) - µm	359.07 ± 125.32 (219.58–595.43)	312.28 ± 117.64 (209.76–506.79)
HUMERUS		
D : Mean ± SD (range) -	1965.35 ± 318.00 (1559.89–2483.95)	1906.94 ± 478.71 (1501.08–3046.54)
d : Mean ± SD (range) - µm	1203.45 ± 112.47 (1013.83–1346.66)	1216.73 ± 220.07 (978.19–1687.38)
MP : Mean ± SD (range) - µm	427.12 ± 152.37 (242.13–783.82)	382.87 ± 172.13 (235.60–750.46)
FIBULA		
D : Mean ± SD (range) -	957.13 ± 152.86 (724.27–1258.75)	957.84 ± 213.83 (772.01–1405.76)
d : Mean ± SD (range) - µm	550.56 ± 64.15 (419.18 9–643.76)	566.85 ± 81.58 (471.65–745.74)
MP : Mean ± SD (range) - µm	227.82 ± 80.39 (140.99–426.74)	213.33 ± 79.59 (124.04–370.31)
RADIUS		
D : Mean ± SD (range) -	974.45 ± 150.76 (789.19–1286.42)	969.40 ± 215.72 (753.37–1446.34)
d : Mean ± SD (range) - µm	563.48 ± 68.49 (426.19–635.90)	580.17 ± 121.14 (442.59–823.21)
MP : Mean ± SD (range) - µm	250.85 ± 72.99 (167.03–430.10)	227.72 ± 64.64 (148.31–341.68)
ULNA		
D : Mean ± SD (range) -	1209.48 ± 289.71 (946.03–1769.84)	1264.44 ± 187.61 (980.15–1599.78)
d : Mean ± SD (range) - µm	699.86 ± 169.50 (558.11–1015.11)	731.92 ± 86.42 (591.42–868.92)
MP : Mean ± SD (range) - µm	306.28 ± 97.50 (219.82–519.66)	309.74 ± 82.14 (220.44–472.55)
PHALANX		
D : Mean ± SD (range) -	664.33 ± 664.33 (496.26–896.46)	639.63 ± 166.00 (490.33–966.75)
d : Mean ± SD (range) - µm	423.64 ± 93.76 (320.73–619.49)	403.88 ± 82.92 (326.36–581.30)
MP : Mean ± SD (range) - µm	160.88 ± 24.43 (130.31–205.51)	163.95 ± 58.71 (98.42–300.78)

bivittatus phalanges prevents accurate age estimation. The value of D/d on the phalanx was 1.47, while the correlation value of SVL versus diameter of the marrow cavity was higher (0.81) than other bones, so the phalanx bone cannot be used for age estimation. This extensive resorption also occurred in the phalanx of *V. niloticus* (De Buffrinil and Castanet, 2000).

The bone that could be used in age estimation on *V. niloticus* was the fibula bone (De Buffrinil and Castanet, 2000) because the bone was stable and had a low extent of resorption. This condition also occurred in the fibula of *V.s. bivittatus*, as indicated by the high resorption value (1.72) and the lowest correlation of SVL versus marrow cavity diameter, which was 0.21 (Table 3, 4). Another phenomenon that was found in the fibula bone but not found in other long tubular bones was the AdL in the endosteal bone in an individual with SVL of 25.0 cm (Figure 4). Since the purpose of this study was to find resting line other than LAG that appeared in the cross section of the long tubular bone *V. s. bivittatus*, we called

Table 3. Linear regression of snout to vent length (SVL, µm) versus measurement of bones, i.e. bone diameter (D, µm), marrow cavity diameter (d, µm), and bone thickness (MP, µm) of juvenile *V.s. bivittatus.* All measurements were converted to log value in analysis. Number of individuals = 21 (10 males; 11 females).

Long tubular bone	Log SVL versus log measurement of bone (D, d, MP)	Linear regression	r^2	p
Femur	SVL vs D	y = 149.49x – 631.59	0.93	0.0001
	SVL vs d	y = 62.73x + 213.97	0.68	0.0001
	SVL vs MP	y = 2.1903x – 6.7253	0.72	0.0001
Tibia	SVL vs D	y = 119.2x – 472.35	0.88	0.0001
	SVL vs d	y = 49,912x + 218.86	0.58	0.0002
	SVL vs MP	y = 2.0428x – 6.1825	0.70	0.0001
Humerus	SVL vs D	y = 141.62x – 607.03	0.90	0.0001
	SVL vs d	y = 50.605x + 302.18	0.62	0.0002
	SVL vs MP	y = 2.2767x – 7.0979	0.78	0.0001
Fibula	SVL vs D	y = 66.253x – 231.58	0.95	0.0001
	SVL vs d	y = 14.295x + 302.53	0.28	0.0131
	SVL vs MP	y = 2.0018x – 6.187	0.78	0.0001
Radius	SVL vs D	y = 0.0659x – 211.83	0.94	0.0001
	SVL vs d	y = 0.0291x + 50.456	0.64	0.0001
	SVL vs MP	y = 0.0195x – 112.02	0.60	0.0001
Ulna	SVL vs D	y = 0.0865x – 316.69	0.92	0.0001
	SVL vs d	y = 0.0378x + 36.75	0.57	0.0002
	SVL vs MP	y = 0.0298x – 226.45	0.82	0.0001
Phalanx	SVL vs D	y = 0.0513x – 268.68	0.94	0.0001
	SVL vs d	y = 0.029x – 107.11	0.81	0.0001
	SVL vs MP	y = 0.013x – 71.205	0.61	0.0004

Table 4. Descriptive statistics on measurement of long tubular bones, i.e. bone diameter (D, µm), marrow cavity diameter (d, µm) and resorption rate value (D/d) of juvenile *V.s. bivittatus* (n = number of individuals; SD = standard deviation).

Long tubular bone	D Mean ± SD (n = 21) µm	d Mean ± SD (n = 21) µm	D/d Mean ± SD (n = 21)
Femur	2051.36 ± 416.91	1339.82 ± 204.82	1.53 ± 0.20
Tibia	1667.05 ± 341.55	1114.67 ± 176.64	1.49 ± 0.15
Humerus	1934.76 ± 401.22	1210.41 ± 173.07	1.60 ± 0.19
Fibula	957.51 ± 182.69	559.09 ± 72.45	1.72 ± 0.26
Radius	971.80 ± 183.04	572.22 ± 97.57	1.71 ± 0.19
Ulna	1235.65 ± 242.07	715.13 ± 134.14	1.74 ± 0.18
Phalanx	651.39 ± 141.71	413.29 ± 86.58	1.47 ± 0.40

the line as the additional resting line (AdL; Figure 4) which appeared in endosteal bone. The AdL appears to be the result of a brief nonannual pause in endosteal bone growth, similar with the findings of Kurita and Toda (2013) which described similar lines within the 'Absorption Zone' of *Goniurosaurus kuroiwae* bone cortices.

The average length of the neonates of *V. salvator* was 5.915 cm, and the range was 4.7–7.7 cm (Thompson and Pianka, 2001). Based on the specimens of this study, in females, the first LAG appeared in an individual with SVL of 18.8 cm and also in another individual with a SVL of 22.2 cm. If the neonate's average SVL was 5.915 cm (Thompson and Pianka, 2001), then the estimated annual increases of SVL lengths were 12.9 cm and 16.3 cm, respectively. However, in an individual with SVL of 25.0 cm, the second LAG appeared, then the estimated increases in the SVL lengths in the second year were 2.8 cm and 6.2 cm, respectively. There was a very short distance between two LAGs and an extensive SVL range between the first and second LAG. The existence of the second LAG is still a question. According to Andrews (1995), the SVL of *V. salvator* in India in the second year was above 40 cm. The second LAG that appeared in the female of *V.s.bivittatus* is believed to be a false LAG because it does not show a complete circle around the bone, as demonstrated by the first LAG. The false LAG is an AdL which appeared in periosteal bone; this line was also found in periosteal bone of *P. interscapularis* (Smirina and Ananjeva, 2017) and *G. gecko* (Kurniati and Phadmacanty, 2022).

In males, an individual with SVL of 19.3 cm had one LAG, but also an individual had an SVL of 22.2 cm. Therefore, after 1 year old and before 2 years old, the increases of SVL in males were 13.8 cm and 16.3 cm, respectively. Based on these observations, there was not much difference in growth rates between males and females in the early juvenile stage of *V.s. bivittatus.* According to Bin Abdul and Bin Abdullah (1998), the growth of wild *V. salvator* in Malaysia was fast from the neonates to 1 year, with SVLs of 160 cm, so the average increase of SVL was 22 cm per year, after which, at SVLs of 200 cm, growth rates were much slower. However, in this study, the first LAG appeared on individuals with SVL 18.8 cm and 19.3 cm. It is possible that the low growth rates on these individuals due to environmental factors, including food deficiency and unfavorable climatic conditions that produced very small annual bone growth increments (Smirina and Tsellarius, 1996).

5. Conclusion

The resorption process from the long tubular bones in *V.s. bivittatus* is started in the early juvenile stage. However, the process in the big tubular bones (femur, tibia, humerus) occurs earlier and faster than those of the process in the small tubular bones (fibula, radius, ulna, phalanx). The fibula bone of *V.s. bivittatus* is a more suitable bone to estimate age using skeletochronology method because the bone has the lowest rate of resorption. The bone measurements (D, d, MP) showed that there was no sexual dimorphism on mid-diaphysis bone size in the juvenile stage of *V.s. bivittatus*. The radial osteon appeared early in the big tubular bones (femur, tibia, humerus) followed by the small tubular bones (radius, ulna); however, in the fibula and the phalanx, the radial osteon was not found even though the SVL got longer. The density of radial osteon increases as the length of SVL and age increase; however, it is not influenced by sex in the early juvenile stage. In step with the rise of SVL, LAGs were prevalent across the sampled specimens, while nonannual AdLs were restricted to a single individual of individual with SVL 25.0 cm; however, only in the fibula bone the AdL appeared in endosteal bone.

Acknowledgments

We are thankful to PT. Mega Citrindo, Jakarta, who donated the specimens for this research. Many thanks are also given to Erick Wiradinata of AIRAI, who financially supported this research. Appreciations are addressed to reviewers and Ronald Lilley for editing the English.

Contribution of authors

HK initiated the study. NLPRP and GS performed the lab work and provided bone samples from the specimens. HK performed the data analysis. HK, NLPRP, and GS contributed equally in the writing of the paper. All the authors read and approved the final manuscript.

Conflicts of interest

The authors declare no conflicts of interest in this study.

References

Andrews HV (1995). Sexual maturation in *Varanus salvator* (laurenti, 1768), with notes on growth and reproductive effort. Herpetological Journal 5: 189-19.

Bennett D (1998). Monitor lizards. Natural history, biology & husbandry. Edition Chimaira. Frankfurt.

Bin Abdul J, Bin Abdullah MA (1988). Growth rate and behaviour of water monitor lizard (*Varanus salvator*) at Sg. Tembeling, Taman Negara. The Journal of Wildlife and Parks 7: 58-66.

Bulbul U, Kurnaz M, Eroglu AI, Koc H, Kutrup B (2016). Age and growth of the red-belied lizard, *Darevskia parvula*. Animal Biology 66: 81-95. https://doi.org/10.1163/15707563-00002489

Castanet J (1994), Age estimation and longevity in reptiles. Gerontology 40: 174-192.

Comas M, Reguera S, Zamora-Camacho FJ, Salvado H, Moreno-Rueda G (2016), Comparison of the effectiveness of phalanges vs humeri and femurs to estimate lizard age with skeletochronology. Animal Biodiversity Conservation 39(2): 237-240.

De Buffrinil V, Castanet J (2000). Age estimation by skeletochronology in the Nile Monitor (*Varanus niloticus*), a highly exploited species. Journal of Herpetology 34 (3): 414-424.

Eden CJ, Whiteman HH, Duobinis-Gray L, Wissinger SA (2007). Accuracy assessment of skeletochronology in the arizona tiger salamander (*Ambystoma tigrinum nebulosum*). Copeia (2): 471-477.

Francillon-Vieillot H, Arntzen JW, Geraudie J (1990). Age, growth and longevity of sympatric *Triturus cristatus, T. marmoratus* and their hybrids (Amphibia, Urodela): a skeletochronological comparison. Journal of Herpetology 24: 13-22.

Frynta D, Frýdlová P, Hnízdo J, Šimková O, Veronika Cikánová V, et al. (2010). Ontogeny of sexual size dimorphism in monitor lizards: males grow for a longer period, but not at a faster rate. Zoological Science 27 (12): 917-923. https://doi.org/10.2108/zsj.27.917

Halliday TR, Verrell PA (1988). Body size and age in amphibians and reptiles. Journal of Herpetology 22 (3): 253-265.

Hammer Ø, Harper DAT, Ryan PD (2001). PAST: Paleontological statistics software package for education and data analysis. Palaeontol Electronica 4: 9.

Koch A, Auliya M, Ziegler T (2010). Updated checklist of living monitor lizards of the world (Squamata:Varanidae). Bonn Zoological Bulletin 57:127-136.

Kumas M, Ayaz D (2014). Age determination and long bone histology in *Stellagama stellio* (Linnaeus, 1758) (Squamata: Sauria: Agamidae) populations in Turkey. Vertebrate Zoology 64 (1): 113-126

Kurita T, Toda M (2013). Validation and application of skeletochronology for age determination of the Ryukyu ground gecko, *Goniurosaurus kuroiwae* (Squamata: Eublepharidae). Asian Herpetological Research 4 (4): 233-241. https://doi.org/10.3724/SP.J.1245.2013.00233

Kurniat H, Phadmacanty NLPR (2022). Age and body growth of the tokay gecko, *Gekko gecko* (Linnaeus, 1758), studied by the skeletochronological method. Russian Journal of Herpetology 29 (3): 161-168. https://doi.org/10.30906/1026-2296-2022-29-3-161-168

Quah E, Lwin K, Cota M, Grismer L, Neang T et al. (2021). *Varanus salvator*. The IUCN Red List of Threatened Species 2021: e.T178214A113138439. https://dx.doi.org/10.2305/IUCN.UK.2021-2.RLTS.T178214A113138439.en

Schneider CA, Rasband WS, Eliceiri KW. (2012). NIH image to mageJ: 25 years of image analysis. Nature Methods 9: 671-675.

Shine R, Harlow PS, Keogh JS, Boeadi (1996). Commercial harvesting of giant lizards: the biology of water monitors *V. salvator* in southern Sumatra. Biological Conservation 77: 125-134.

Shine R, Ambariyanto, Harlow PS, Mumpuni (1998). Ecological traits of commercially harvested water monitors, *V. salvator*, in northern Sumatra. Wildlife Research 25: 437-447.

Sinsch U (2015). Review: skeletochronological assessment of demographic life-history traits in amphibians, Herpetological Journal 25 (1): 5-13.

Smirina E, Ananjeva N (2017). On the longevity, growth and reproductive characteristics of Lichtenstein's Toadhead Agama, *Phrynocephalus interscapular* Lichtenstein, 1856 (Agamidae, Sauria). Amphibia-Reptilia 38: 31-39. https://doi.org/10.1163/15685381-00003080

Smirina EM, Tsellarius AY (1996). Aging, longevity, and growth of the desert monitor lizard (*Varanus griseus* Daud.). Russian Journal of Herpetology 3 (2): 130-142.

Smirina EM, Tsellarius AY (1998). Vital bone marking of desert monitor (*Varanus griseus* Daud.) in nature. Russian Journal of Herpetology 5 (2): 156-159.

Thompson GG, Pianka ER (2001). Allometry of clutch and neonate sizes in monitor lizards (Varanidae: *Varanus*). Copeia (2): 443-458.

Uzum N, Ilgaz C, Kumlutas Y, Gumus C, Avci A (2014). The body size, age structure, and growth of Bosc's fringe-toed lizard, *Acanthodactylus boskianus* (Daudin, 1802). Turkish Journal of Zoology 38: 383-388. https://doi.org/10.3906/zoo- 1307-1

Uzum N, Avci A, Kumlutas Y, Bese, N, Ilgaz C (2015). The first record of structure and body size of the Suphan Recerunner, *Eremias suphani* Basoglu & Hellmich, 1968. Turkish Journal of Zoology 39: 513-518. https://doi.org/10.3906/zoo- 1408-39

Uzum N, Ilgas C, Avci A, Candan K, Guler H et al. (2018). Comparison of the body size and age structure of Lebanon lizard, *Phoenicolacerta laevis* (Gray, 1838) at different altitudes in Turkey. Vertebrate Zoology 68 (1): 83-90.

Wagner A, Schabetsberger R, Sztatecsny M, Kaiser R (2011). Skeletochronology of phalanges underestimates the true age of long-lived Alpine newts (*Ichthyosaura alpestris*). Herpetological Journal 21: 145-148.

Woodward HN, Padian K, Lee AH (2013). Skeletochronology. In: Padian K, Lamm ET, editors. Bone Histology of Fossil Tetrapods: Advancing Methods, Analysis, and Interpretation. California Scholarship Online. Oakland, CA. pp. 195-215. https://doi.org/10.1525/california/9780520273528.003.0007